# 3D FINITE ELEMENT ANALYSIS OF A COMPACT TENSION SHEAR–SPECIMEN UNDER IN–PLANE MIXED–MODE LOADING

F.–G. Buchholz *, P. Diekmann **, H.A. Richard *, H. Grebner **

A 3D fracture analysis of a compact tension shear (CTS)–specimen is presented, achieved by the aid of the finite element method (FEM) and the generalized modified virtual crack closure– and the equivalent domain integral method. It is shown that by in–plane mixed–mode loading conditions of the CTS–specimen variable mixed–mode I, II and III crack tip conditions are created along the straight crack front through the thickness of the specimen. It is found that the energy release rate $G_I$ decreases distinctly adjacent to the free surface of the specimen, whereas $G_{II}$ and the additionally induced $G_{III}$ show remarkably increasing values there.

## INTRODUCTION

Mixed–mode fracture is an important subject in fracture mechanics because mixed– mode fracture conditions do occur in engineering practice under various geometrical– and loading conditions. In order to cover the full range of combined in–plane tension/ shear loadings in experimental fracture mechanics the compact tension shear (CTS)–specimen and the special loading device (Fig. 1) has been designed by RICHARD /1/. In this paper finite element– and fracture analysis results are presented for 3D–models of the CTS–specimen under different in–plane tension/shear loadings. The detailed investigation will show that by in–plane mixed–mode loading conditions additional 3D– and out of plane effects arise at the crack front due to the finite thickness of the specimen (t = 10–20mm). This kind of complex 3D fracture behavior can be analysed by 3D generalizations of the numerically highly effective Modified Virtual Crack Closure Integral (MVCCI)– and the Equivalent Domain Integral (EDI)–method, which both provide simultaneously the separated energy release rates $G_i$ (a, z/t), i = I, II, III for linear elastic material behavior.

* Universität–GH–Paderborn, D–4790 Paderborn, FRG
** Gesellschaft für Reaktorsicherheit (GRS), D–5000 Köln, FRG

## 3D MVCC– AND EDI–METHOD

Generalizations of the straight forward and numerically effective VCCI–methods from 2D– to 3D–problems have been given by BUCHHOLZ et al /2,3/ and SHIVAKUMAR et al /4/ with slightly different approaches. The successful applications cover various 3D–problems including surface cracks in different structures and debonding processes in 3D fibre/matrix composite cylinders, where all fracture modes I, II and III are created along interface crack fronts. For the present analysis of the 3D CTS–specimen the 3D MVCCI–method is used as formulated for 20–node volume elements by SHIVAKUMAR /4/. For details of the method reference has to be given to /4/

The same holds for the EDI–method given by NIKISHKOV and ATLURI in /5/. The EDI–method for 3D–problems is a numerically highly efficient extension of the 3D virtual crack extension (VCE)–method by DELORENZI /6/. In combination with the decomposition of the stress, strain and displacement fields into mode I, II and III components /4/ the energy release rates $G_i$ (a, z/t), i = I, II, III can be computed for general mixed–mode cases in 3D and furthermore for nonlinear and elastic–plastic material behavior. A FE–postprocessor programmed by DIEKMANN /7/ on the basis of /5,6/ has been used to achieve the EDI–results for the 3D CTS–specimen.

## CTS–SPECIMEN AND 3D FE–MODEL

In Fig. 1 the CTS–specimen and the loading device are displayed as mounted together in a standard tensile testing machine.By aid of the special loading device various in–plane loading conditions can be created, reaching from pure tension ($\alpha$ = 0 deg.) via in–plane tension/shear (0 < $\alpha$ < 90 deg.) to pure in–plane shear loading ($\alpha$ = 90 deg.).

Figure 2 shows the 3D FE–model of the CTS–specimen which has 6966 degrees of freedom and is assembled from 404 20–node volume elements. Away from the crack front the model contains one element through the thickness ($0 \leq z/t \leq 0.5$), whereas mesh refinements are incorporated next to the straight crack front (a = const.) and adjacent to the free surface ($z/t \rightarrow 0.5$).

## DISCUSSION OF FRACTURE ANALYSIS RESULTS

In Fig. 3 the deformed FE–mesh of the CTS–specimen is given for pure tension loading and clearly the correlated mode I crack opening is to be seen. The quantitative results in form of the normalized energy release rate $G^n$ (a, $z/t) \equiv G_I^n = G_I/[(F/wt)\cdot a]$ show slightly decreasing values for $0 \leq z/t \leq 0.4$, with coinciding graphs for both methods (MVCCI, EDI), but stronger decreasing curves adjacent to the free surface of the specimen ($z/t \rightarrow 0.5$). Probably the slightly curved crack fronts, which are frequently found in mode I fatigue experiments, are due to this 3D–effect to some extend, because of

reduced fatigue crack growth rates for $z/t \to 0.5$. As another obvious 3D–effect it should be mentioned that the 3D G1N–graph does not meet the 2D limit case values, which are given in Fig. 3 too from 2D reference solutions /1/. At the free surface ($z/t = 0.5$) the G1N–graph ends distinctly below the 2D plane stress value and in the plane of symmetry ($z/t = 0$) it still exceeds the 2D plane strain value, which is reasonable for this specimen with only t = 10 mm thickness.

More complex is the situation if the CTS–specimen is subjected to in–plane tension/shear loadings for $0 < \alpha < 90$ deg.. In the 2D case this creates plane mixed–mode I and II conditions at the crack tip, which are visible in Fig. 4 through the crack face displacements of the deformed 3D FE–mesh of the specimen. Moreover it is indicated by Fig. 4 that the level of mode I loading at the crack front is remarkably lower now, but the course of the G1N–graph with z/t is about the same as for $\alpha = 0$ deg. The additional mode II loading (G2N–graph) is rather constant for $0 \leq z/t \leq 0.4$, but shows slightly increasing values for $z/t \to 0.5$. Furthermore it can be concluded from the G3N–graph in Fig. 4, that by the in–plane mixed–mode loading of the specimen also some out of plane shear effect (mode III) is created at the crack front adjacent to the free surface ($z/t \geq 0.3$). Superposition of all effects results in the total energy release rate (GGN–graph) as given in Fig. 4 too.

Most clearly the 3D– and out of plane effects are to be seen in Fig. 5 for pure in–plane shear loading of the CTS–specimen. Here a remarkable increase can be observed for the G3N–graph with $z/t \to 0.5$, what is also found for mode II (G2N–graph) and consequently for the total energy release rate too (GGN–graph). Furthermore from Fig. 5 it can be seen, that the excellent agreement between both fracture analysis methods (MVCCI, EDI) is slightly affected for $z/t \to 0.5$, because the local 3D– and out of plane effects with $z/t \to 0.5$ are experienced more in detail by the EDI–method. This tendency of the EDI–results agree well with findings in /8/, obtained by those variants of the VCC– and MVCCI–methods, which define the energy release rates for each plane of nodal points per element /2,3/. Furthermore these results are supported by findings in /9/, obtained by special 3D hybrid crack front elements for a similar problem, but on the other hand for $z/t < 0.2$ the $K_{III}$–graphs in /9/ show courses which do not agree with the corresponding MVCCI– and EDI–findings here. Some further improvement should be attained for the mode decomposition part of the EDI–postprocessor /7/, because sometimes $G3N < 0$ is obtained for small numbers and the total energy release rate results show minor deviations from each other if calculated with – or without mode decomposition.

## REFERENCES

(1) Richard, H.A.: Bruchvorhersagen bei überlagerter Normal– und Schubbeanspruchung von Rissen. VDI–Forschungsheft 631, VDI–Verlag, Düsseldorf, 1985

(2) Buchholz, F.–G., Schulte–Frankenfeld, N., Meiners, B.: Fracture Analysis of Mixed–Mode Failure Processes in a 3D Fibre/Matrix Composite Cyliner. In Proc. 6th Int. Conf. on Composite Materials

(ICCM–6), Vol. 3, (Eds. F.L. Matthews et al), Elsevier Appl. Science Publ., London, 1987, 3.417–3.428

(3) Buchholz, F.–G., Grebner, H., Dreyer, K.–H., Krome, H.: 2D– and 3D–Applications of the Improved and Generalized Modified Crack Closure Integral Method. In Computational Mechanics 88, Vol. 1, (Eds. S.N. Atluri, G., Yagawa), Springer Verl., New York, 1988, 14.i.1–14.i.4

(4) Shivakumar, K.N., Tan, P.W., Newman, J.C., Jr.: A Virtual Crack–Closure Technique for Calculating Stress Intensity Factors for Cracked Three Dimensional Bodies. Int. J. Fracture 36 (1988), R43–R50

(5) Nikishkov, G.P., Atluri, S.N.: Calculation of Fracture Mechanics Parameters for an Arbitrary 3D Crack by the Equivalent Domain Integral Method. Int. J. Num. Meth. Engng. 24 (1987), 1801–1821

(6) DeLorenzi, H.G.: Energy Release Rate Calculations by the Finite Element Method. Eng. Fract. Mech. 21 (1985), 129–143

(7) Diekmann, P.: 3D EDI–Postprozessor, GRS–Report

(8) Buchholz, F.–G., Kurtenbach, V., Schröder, S., Umlauf, B., Richard, H.A.: 3D Finite Element Analyse einer CTS–Probe unter ebener Zug/ - Schubbelastung. Proc. 22. Vortragsveranstaltung des DVM–Arbeitskreises "Bruchvorgänge". Edt. by DVM, Berlin, 1990, 299–309

(9) Richard, H.A., Kuna, M.: Theoretical and Experimental Study of Superimposed Fracture Modes I, II and III. Engng. Frac. Mech. 35 (1990), 949–960

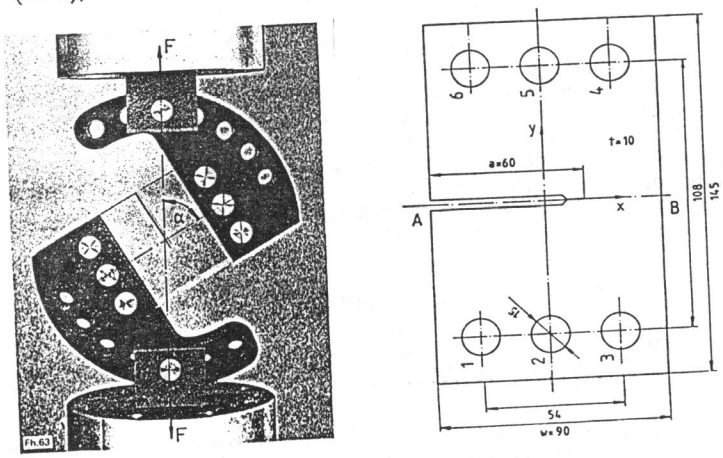


Fig. 1 Loading device and CTS–specimen (in–plane tension/shear loading, $\alpha = 60$ deg., a/w = 2/3, w = 90, d = 68, t = 10mm, F = 40kN)

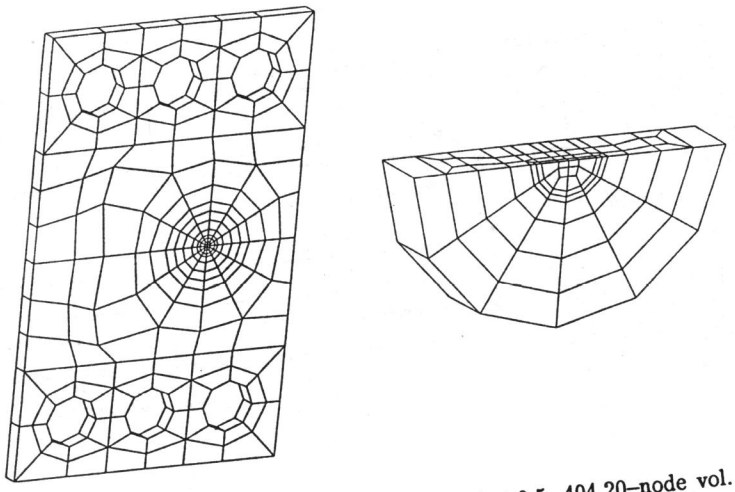

Fig. 2 3D FE–model of the CTS–spec. ($0 \leq z/t \leq 0.5$, 404 20–node vol. el., 6966 DOF, $E = 80{,}000.N/mm^2$, $\lambda = 0.3$)

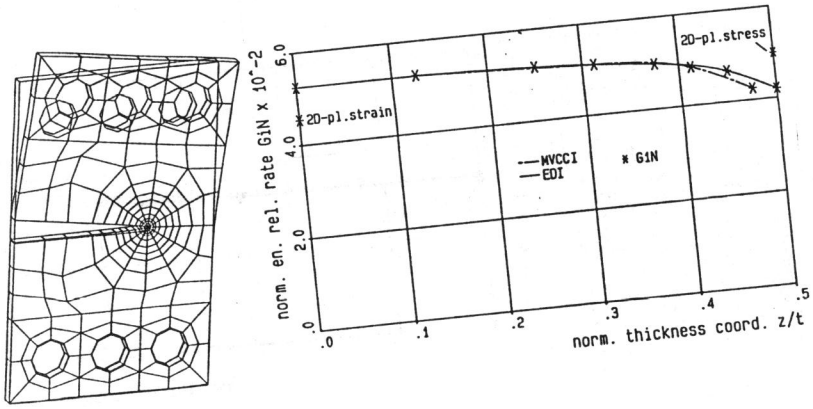


Fig. 3 Deformed 3D FE–model of the CTS–specimen under pure tension loading ($\alpha$=0 deg.) and correlated norm. energy release rates (ERR).

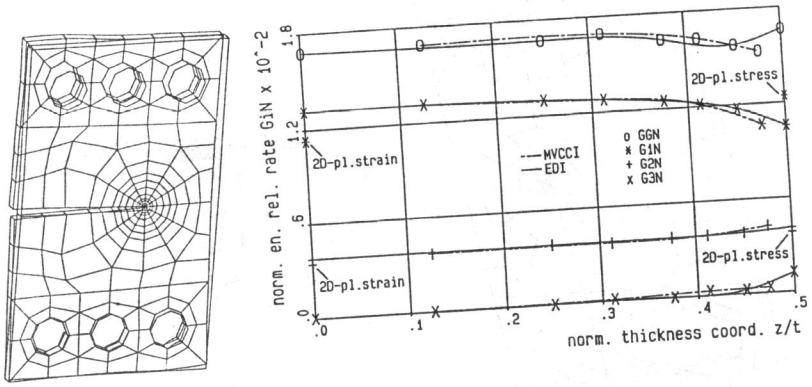


Fig. 4 Deformed 3D FE–model of the CTS–specimen under in–plane tension/shear loading ($\alpha$=60 deg.) and correlated norm. ERR.

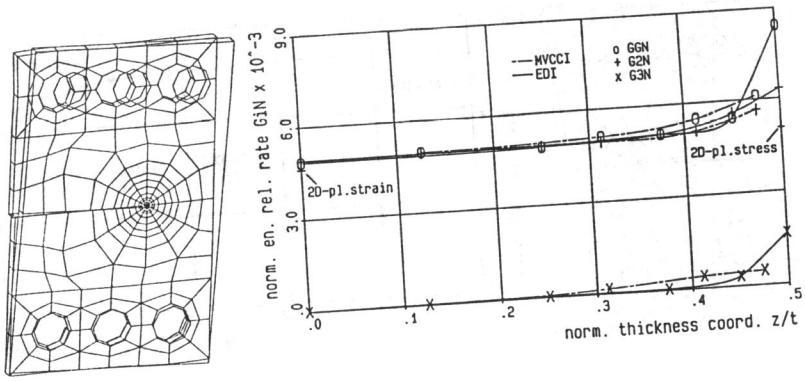


Fig. 5 Deformed 3D FE–model of the CTS–specimen under pure in–plane shear loading ($\alpha$=90 deg.) and correlated norm. ERR.